Experimental and Modeling Study of Catalytic Reaction of Glucose Isomerization: Kinetics and Packed-Bed Dynamic Modeling

Asghar Molaei Dehkordi, Iman Safari, and Muhammad M. Karima
Dept. of Chemical and Petroleum Engineering, Sharif University of Technology, Tehran, Iran

DOI 10.1002/aic.11460
Published online March 26, 2008 in Wiley InterScience (www.interscience.wiley.com).

The kinetics and equilibrium of isomerization reaction of D-glucose to D-fructose have been investigated using a commercial immobilized glucose isomerase (IGI), Sweetzyme type IT®, in a batch stirred-tank reactor. The batch experimental data were used to model the reaction kinetics using the well-known Michaelis–Menten rate expression. The kinetic model was utilized in a dynamic-mathematical model for a packed-bed reactor to predict the concentration profiles of D-glucose and D-fructose within the reactor. The experimental results for the fractional conversion of D-glucose in the packed-bed reactor of IGI catalyst indicated that the model prediction of the transient and steady-state performance of the packed-bed reactor was satisfactory and as such could be used in the design of a fixed-bed IGI catalytic reactor. Moreover, the influences of axial mixing term, particle Re *number, and axial peclet number (*Pe_a*) on the performance capability of the packed-bed reactor of IGI catalyst were investigated.*
 AIChE J, 54: 1333–1343, 2008
Keywords: kinetics, packed bed, mathematical modeling, transient response, dynamic simulation, enzyme, glucose isomerase

Introduction

Solid–liquid enzyme reactions constitute important processes in biochemical industries. Among the latter, the isomerization of glucose to fructose is one of the most widely used processes in the food industry in producing dietetic "light" foods and drinks, because it improves the sweetening, color, and hygroscopic characteristics in addition to reducing viscosity. Also, fructose is about 75% sweeter than sucrose, is absorbed more slowly than glucose, and is metabolized without the intervention of insulin. For all these reasons, this process is widely studied both with cells and with enzymes, both free and immobilized.[1–15] From the perspective of chemical kinetics, isomerization of glucose to fructose is a reversible reaction, with an equilibrium constant of approximately unity at 55°C.[16] The heat of reaction is on the order of 5 kJ/mol[16] and, consequently, the equilibrium product contains roughly a 1:1 ratio of glucose to fructose that does not change appreciably with temperature, such that at 55°C the fructose content at equilibrium is 50%, and at higher temperatures such as 60, 70, 80, and 90°C is 50.7, 52.5, 53.9, and 55.6%, respectively. However, increasing temperature decreases stability and the enzyme half-life and therefore productivity. Most industrial plants run at 58–60°C, a temperature with low risk for microbial contamination.

The process was originally carried out in batch reactors with soluble enzymes. It was later extended to one involving immobilized glucose isomerase (IGI), which is of interest to us in the present work. In addition to the aforementioned batch reactors, there are various types of enzyme reactors, including continuous stirred tank reactors, fixed-bed reactors, simulated moving beds,[17] and fluidized-bed reactors. In the fixed- and fluidized-bed reactors, the immobilized enzymes are used with different shapes including cylindrical and

Correspondence concerning this article should be addressed to A.M. Dehkordi at amolaeid@sharif.edu.

spherical pellets. Because the microporous particles provide a large surface area and that packing such particles in a tubular reactor is rather straightforward, tubular packed-bed reactors consisting of IGI are extensively used. Isomerization of glucose to fructose is normally carried out in multiple tubular packed-bed reactors in parallel lines, with an isomerization time ranging from 0.5 to 4 h.[16]

The main objectives of the present work were (1) to investigate the kinetics of glucose to fructose isomerization by IGI (Sweetzyme type IT®); (2) to model and simulate dynamically packed-bed reactor using the kinetic parameters obtained by batch experimental runs; and (3) to validate the dynamic packed-bed model through experimental data.

Theory

Reaction kinetics

Glucose–fructose enzymatic isomerization is a reversible reaction and is normally given by the following expression:

$$\mathrm{G} + \mathrm{E} \underset{k_{-1}}{\overset{k_1}{\rightleftarrows}} \mathrm{GE} \underset{k_{-2}}{\overset{k_2}{\rightleftarrows}} \mathrm{F} + \mathrm{E} \tag{1}$$

where G, E, and F represent glucose, enzyme, and fructose, respectively, and GE is an intermediate complex formed during the reaction. According to the reversible modified Michaelis–Menten mechanism,[2,8,18,19] the reaction rate is given by

$$R = -\frac{1}{W}\frac{d[\overline{\mathrm{G}}]}{dt} = \frac{V_\mathrm{m}[\overline{\mathrm{G}}]}{K_\mathrm{m} + [\overline{\mathrm{G}}]} \tag{2}$$

with

$$[\overline{\mathrm{G}}] = [\mathrm{G}] - [\mathrm{G}]_\mathrm{e}, \quad [\mathrm{G}]_0 = [\mathrm{G}] + [\mathrm{F}] = [\mathrm{G}]_\mathrm{e} + [\mathrm{F}]_\mathrm{e} = (1 + K_\mathrm{e})[\mathrm{G}]_\mathrm{e} = \left(1 + K_\mathrm{e}^{-1}\right)[\mathrm{F}]_\mathrm{e} \tag{3}$$

$$K_\mathrm{m} = \frac{k_\mathrm{mf}k_\mathrm{mg}}{k_\mathrm{mf} - k_\mathrm{mg}}\left[1 + \left(\frac{1}{k_\mathrm{mg}} + \frac{K_\mathrm{e}}{k_\mathrm{mf}}\right)[\mathrm{G}]_\mathrm{e}\right] \tag{4}$$

$$V_\mathrm{m} = \left[1 + K_\mathrm{e}^{-1}\right]\frac{k_\mathrm{mf}v_\mathrm{mg}}{k_\mathrm{mf} - k_\mathrm{mg}} \tag{5}$$

$$K_\mathrm{e} = \frac{[\mathrm{F}]_\mathrm{e}}{[\mathrm{G}]_\mathrm{e}} = \frac{X_\mathrm{e}}{1 - X_\mathrm{e}} = \frac{v_\mathrm{mg}k_\mathrm{mf}}{v_\mathrm{mf}k_\mathrm{mg}} \tag{6}$$

where v_mg, v_mf, k_mg, and k_mf are the maximum reaction rate for glucose to fructose, the maximum reaction rate for fructose to glucose, the Michaelis–Menten constant for glucose to fructose reaction, and the Michaelis–Menten constant for fructose to glucose reaction, respectively, and X_e is the equilibrium fractional conversion of glucose. Integrating Eq. 2 gives

$$t = \frac{1}{W}\left[\frac{[\overline{\mathrm{G}}]_0 - [\overline{\mathrm{G}}]}{V_\mathrm{m}} + \frac{K_\mathrm{m}}{V_\mathrm{m}}\ln\frac{[\overline{\mathrm{G}}]_0}{[\overline{\mathrm{G}}]}\right] \tag{7}$$

Thus, by introducing the values of v_mg, v_mf, k_mg, and k_mf to Eqs. 4 and 5 together with Eq. 7, one can easily evaluate the fractional conversion of glucose at any given time for various initial concentrations of glucose.

The conventional method reported in the literature for determining v_mg, v_mf, k_mg, and k_mf is that experiments with feed solution containing either glucose or fructose should be carried out. By estimating the initial rates of the glucose to fructose and vice versa, these parameters can be determined using the Lineweaver–Menten equation.[20] However, one can evaluate these four key parameters (i.e., v_mg, v_mf, k_mg, and k_mf) by carrying out just experiments for glucose to fructose reaction. Rubio et al. have rewritten the rate of reaction as follows[21]:

$$R = -\frac{1}{W}\frac{d[\mathrm{G}]}{dt} = K_\mathrm{r}\frac{(X_\mathrm{e} - X)}{1 + KX} \tag{8}$$

with

$$K_\mathrm{r} = \frac{v_\mathrm{mg}\left(1 + K_\mathrm{e}^{-1}\right)}{k_\mathrm{mg} + [G]_0}[\mathrm{G}]_0 \tag{9}$$

and

$$K = \frac{[\mathrm{G}]_0\left[\left(\frac{k_\mathrm{mg}}{k_\mathrm{mf}}\right) - 1\right]}{k_\mathrm{mg} + [\mathrm{G}]_0} \tag{10}$$

where K_e, W, and X denote the equilibrium constant, catalyst loading, and the fractional conversion of glucose, respectively. Integrating Eq. 8 gives the following relation:

$$t = \frac{[\mathrm{G}]_0}{W}\frac{KX_\mathrm{e} + 1}{K_\mathrm{r}}\ln\left(\frac{X_\mathrm{e}}{X_\mathrm{e} - X}\right) - \frac{[\mathrm{G}]_0}{W}\frac{K}{K_\mathrm{r}}X \tag{11}$$

To evaluate K and K_r as a function of initial concentration of glucose, one can plot $tW/(X[\mathrm{G}]_0)$ against $1/X \ln[X_\mathrm{e}/(X_\mathrm{e} - X)]$ for various constant initial concentrations. Note that, the equilibrium fractional conversion of glucose (X_e) can be determined experimentally by conducting long enough experimental runs. On the other hand, the inversion of Eqs. 9 and 10 yields

$$\frac{1}{K_\mathrm{r}} = \frac{k_\mathrm{mg}}{v_\mathrm{mg}\left(1 + \frac{1}{K_\mathrm{e}}\right)}\frac{1}{[\mathrm{G}]_0} + \frac{1}{v_\mathrm{mg}\left(1 + \frac{1}{K_\mathrm{e}}\right)} \tag{12}$$

$$\frac{1}{K} = \frac{k_\mathrm{mg}}{\left[\left(\frac{k_\mathrm{mg}}{k_\mathrm{mf}}\right) - 1\right]}\frac{1}{[\mathrm{G}]_0} + \frac{1}{\left[\left(\frac{k_\mathrm{mg}}{k_\mathrm{mf}}\right) - 1\right]} \tag{13}$$

Now, by plotting $1/K$ against $1/[\mathrm{G}]_0$ one can easily evaluate k_mg and k_mf, and finally plotting $1/K_\mathrm{r}$ against $1/[\mathrm{G}]_0$, v_mg could be determined. Having the value of K_e and using Eq. 6, v_mf could be subsequently determined.

Packed-bed modeling

To model packed-bed reactor, the following essential assumptions were considered:

(1) Superficial velocity is high enough so that the external mass-transfer resistance is not dependent on velocity. Lee et al. showed that the critical superficial velocity is 0.1 cm/s.[22] Hence, at superficial velocities higher than this critical value, the external mass-transfer resistance may be considered the same for both the packed bed and the batch experimental runs carried out at a high-enough stirrer speed.

(2) Effectiveness factor is only slightly dependent on bulk glucose concentration.[9,23,24] Thus, the apparent kinetic parameters evaluated by batch experimental runs may be used

in the packed-bed reactor, as the true effectiveness factor was taken into consideration. This assumption is valid when the concentration used for batch experimental runs is the same as those used for packed-bed reactors. Moreover, Pallazi and Converti showed that intraparticle mass-transfer resistance only becomes rather significant for $d_p = 2$ mm, and that the effectiveness factor approaches 1 for $d_p = 0.4$ mm.[9]

(3) Axial dispersion is considered, whereas radial dispersion is neglected.

(4) The system is isothermal.

(5) Fresh catalyst is used, and the time required for running the packed bed reactor is short enough, so that the deactivation is negligible.

Mass balance applied to the concentration of glucose in liquid phase is given by

$$\frac{\partial[\mathrm{G}]}{\partial t} = D_\mathrm{L}\frac{\partial^2[\mathrm{G}]}{\partial z^2} - U_0\frac{\partial[\mathrm{G}]}{\partial z} - R \tag{14}$$

where R, D_L and U_0 denote the glucose reaction rate, axial dispersion coefficient, and the superficial feed velocity, respectively. Note that R is the observed rate of reaction defined by K_m and V_m that are apparent parameters evaluated through the batch experimental runs. Combining Eqs. 2 and 14 and considering the bed porosity (ε) results in the following equation

$$\frac{\partial[\mathrm{G}]}{\partial t} = D_\mathrm{L}\frac{\partial^2[\mathrm{G}]}{\partial z^2} - U_0\frac{\partial[\mathrm{G}]}{\partial z} - \frac{V_\mathrm{m}[\overline{\mathrm{G}}]}{K_\mathrm{m}+[\overline{\mathrm{G}}]}\frac{\rho_\mathrm{p}(1-\varepsilon)}{\varepsilon} \tag{15}$$

where ρ_p is catalyst particle density. This governing equation is subject to the following initial and boundary conditions:

$$[\mathrm{G}] = 0\,; \quad t = 0, z \tag{16}$$

$$-D_\mathrm{L}\frac{\partial[\mathrm{G}]}{\partial z} + U_0[\mathrm{G}] = U_0[\mathrm{G}]_0 \quad t > 0,\ z = 0 \tag{17}$$

$$\frac{\partial[\mathrm{G}]}{\partial z} = \frac{\partial[\overline{\mathrm{G}}]}{\partial z} = 0\,; \quad t > 0,\ z = L \tag{18}$$

where z and L are the z-direction along the packed bed reactor and the height of the reactor, respectively. By introducing the following dimensionless variables

$$\tau = \frac{tU_0}{L\varepsilon}, \quad \xi = \frac{z}{L} \tag{19}$$

Equations 15–18 can be rewritten as follows:

$$\frac{\partial[\overline{\mathrm{G}}]}{\varepsilon\partial\tau} = \frac{D_\mathrm{L}}{LU_0}\frac{\partial^2[\overline{\mathrm{G}}]}{\partial\xi^2} - \frac{\partial[\overline{\mathrm{G}}]}{\partial\xi} - \frac{V_\mathrm{m}[\overline{\mathrm{G}}]}{K_\mathrm{m}+[\overline{\mathrm{G}}]}\frac{\rho_\mathrm{p}L(1-\varepsilon)}{U_0\varepsilon} \tag{20}$$

subject to:

$$[\overline{\mathrm{G}}] = -[\mathrm{G}]_\mathrm{e}\,; \quad \tau = 0\,,\ \xi \tag{21}$$

$$-\frac{D_\mathrm{L}}{U_0L}\frac{\partial[\overline{\mathrm{G}}]}{\partial\xi} + [\overline{\mathrm{G}}] = [\mathrm{G}]_0 - [\mathrm{G}]_\mathrm{e} = [\overline{\mathrm{G}}]_0;\ \tau > 0,\ \xi = 0 \tag{22}$$

$$\frac{\partial[\overline{\mathrm{G}}]}{\partial\xi} = 0\,; \quad \tau > 0,\ \xi = 1 \tag{23}$$

The similar analysis leads to the following equation for the fructose concentration.

$$\frac{\partial[\mathrm{F}]}{\varepsilon\partial\tau} = \frac{D_\mathrm{L}}{LU_0}\frac{\partial^2[\mathrm{F}]}{\partial\xi^2} - \frac{\partial[\mathrm{F}]}{\partial\xi} + \frac{V_\mathrm{m}[\overline{\mathrm{G}}]}{K_\mathrm{m}+[\overline{\mathrm{G}}]}\frac{\rho_\mathrm{p}L(1-\varepsilon)}{U_0\varepsilon} \tag{24}$$

subject to:

$$[\mathrm{F}] = 0\,; \quad \tau = 0,\ \xi \tag{25}$$

$$-\frac{D_\mathrm{L}}{U_0L}\frac{\partial[\mathrm{F}]}{\partial\xi} + [\mathrm{F}] = [\mathrm{F}]_0 = 0; \quad \tau > 0,\ \xi = 0 \tag{26}$$

$$\frac{\partial[\mathrm{F}]}{\partial\xi} = 0\,; \quad \tau > 0,\ \xi = 1 \tag{27}$$

To obtain the concentration profile of glucose and fructose within the packed-bed reactor, Eqs. 20 and 24 along with their initial and boundary conditions should be solved. In the present investigation, the governing equations were solved numerically using the finite-difference method.

Experimental

Chemicals

All chemicals used in the present study were of analytical grade; D-glucose in crystalline form was provided by Merck Co. (Germany). The immobilized enzyme, Sweetzyme IT, was provided as a gift by Novo Nordisk (Iran). The IGI enzyme particles were of cylindrical shape, with 0.2- to 0.4-mm diameter, 1- to 1.5-mm length, and a particle density of 3300 kg/m^3. The dry specific activity of the IGI enzyme was reported to be 450 IGIU/g by the manufacturer. The distilled water used was with conductivity ≤ 3 μS/cm.

Method of analysis

Fructose and glucose concentrations were determined by HPLC (Waters, refractive index detector 2410). The sugar pack$^{\mathrm{TM}}$1 column was used with deionized water as the mobile phase at a flow rate of 0.34 mL/min. The HPLC detector was calibrated by introducing known samples of D-glucose and D-fructose solutions. The regression coefficient of the calibration curve of the detector was 0.996.

Viscosity of feed solutions at 60°C and at various concentrations was determined by a viscometer (Boorkfield LVSVE 230), and the density of these solutions was determined by a density meter (Anton Paar DMA 38).

Experimental apparatus

Batch Stirred-Tank Reactor. The batch reactor was a 500-mL jacketed-stirred tank reactor. The reactor temperature was adjusted by means of hot water. The heating system was able to adjust the temperature of the reactor with the accuracy of ±1°C. Two connections located on the top of the reactor were provided (1) to introduce the desired amount of fresh catalyst to the reactor at the start of each experimental run; and (2) to withdraw samples from the reactor. The impeller was of flat-blade turbine type made of stainless steel (SS), and its rotation speed was adjusted from 100 to 1000 rpm by a variable-speed electric motor.

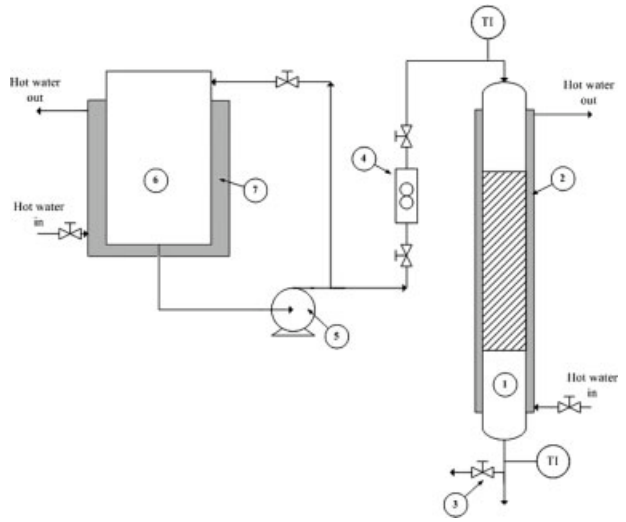

Figure 1. Experimental set up.

(1) packed-bed reactor; (2) hot water jacket; (3) sampling valve; (4) rotameter; (5) stainless steel feed pump; (6) stainless steel feed vessel; (7) hot water jacket.

Packed Bed Reactor. The flow diagram of the experimental setup, shown in Figure 1, consisted of the following parts: packed-bed reactor (1) equipped with a hot water jacket (2), where the dimensions of the packed-bed reactor were of 2 cm diameter (d_b) and 60 cm working height (L); sampling valve (3); rotameter (4); feed pump made of SS (5); feed vessel (6) equipped with jacket (7) made of SS.

Experimental procedures

The D-Glucose solution was prepared by dissolving the required amount of D-glucose in a solution containing 2.465 g $MgSO_4 \cdot 7H_2O$ per liter of deionized water to stabilize the enzyme; the pH of the solution was adjusted at 7.5 by Na_2CO_3. Because oxygen in the syrup inactivates the enzyme and is responsible for increased formation of secondary products during isomerization, a low oxygen tension thus has to be achieved by adding Na_2SO_3.

Batch Experimental Runs. In each experimental run, the feed solution with desired volume, concentration, temperature, and pH was fed to the reactor. Afterward, the impeller speed was adjusted at 700 rpm and the temperature of the reactor was kept at 60°C, and then the desired amount of IGI catalyst was suddenly added to the reactor. This time was considered as the starting time of the reaction. During the course of the reaction, samples were taken through the sampling connection by means of a syringe equipped with a filter to separate the catalyst. The progress of the reaction within the sampling bottle was ceased by adding sulfuric acid solution. Analysis of the samples was performed by the aforementioned analytical method for the glucose–fructose concentrations.

Table 1. Operating Conditions of Batch Experimental Runs

Number of runs	16
Operating temperature (°C)	60 ± 1
pH of glucose solutions	7.5
Initial concentration of glucose (kmol/m^3)	0.10–1.25
Catalyst loading (g/L)	5–20
Duration of each experimental run (min)	120

Table 2. Operating Conditions of Packed-Bed Experimental Runs

Number of runs	16
Operating temperature (°C)	60 ± 1
pH of glucose solutions	7.5
Inlet concentration of glucose (kmol/m^3)	0.10–1.10
Flow rate (L/h)	2.50–16.50
Bed porosity (ε)	0.36
Bed diameter, d_b (m)	0.02
Working bed height, L (m)	0.60

For each data point, the experimental run was repeated at least two times, and thus each data point was determined based on the mean value of at least two measurements of glucose–fructose concentrations with a standard deviation of 1–2%. The operating conditions of all batch experimental runs are presented in Table 1.

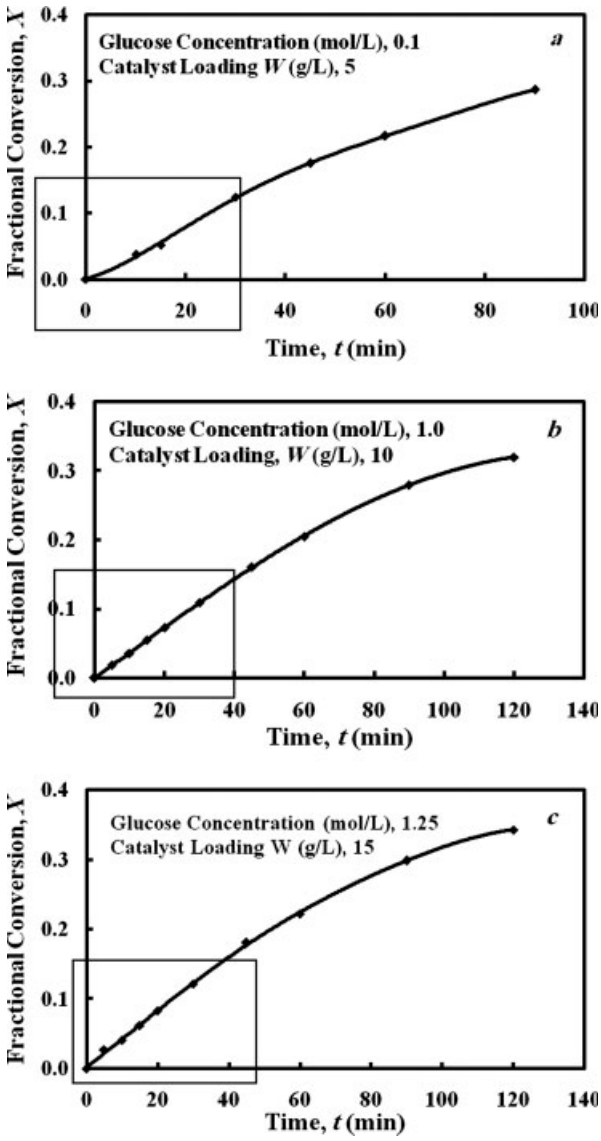

Figure 2. Variations of fractional conversion of glucose with time.

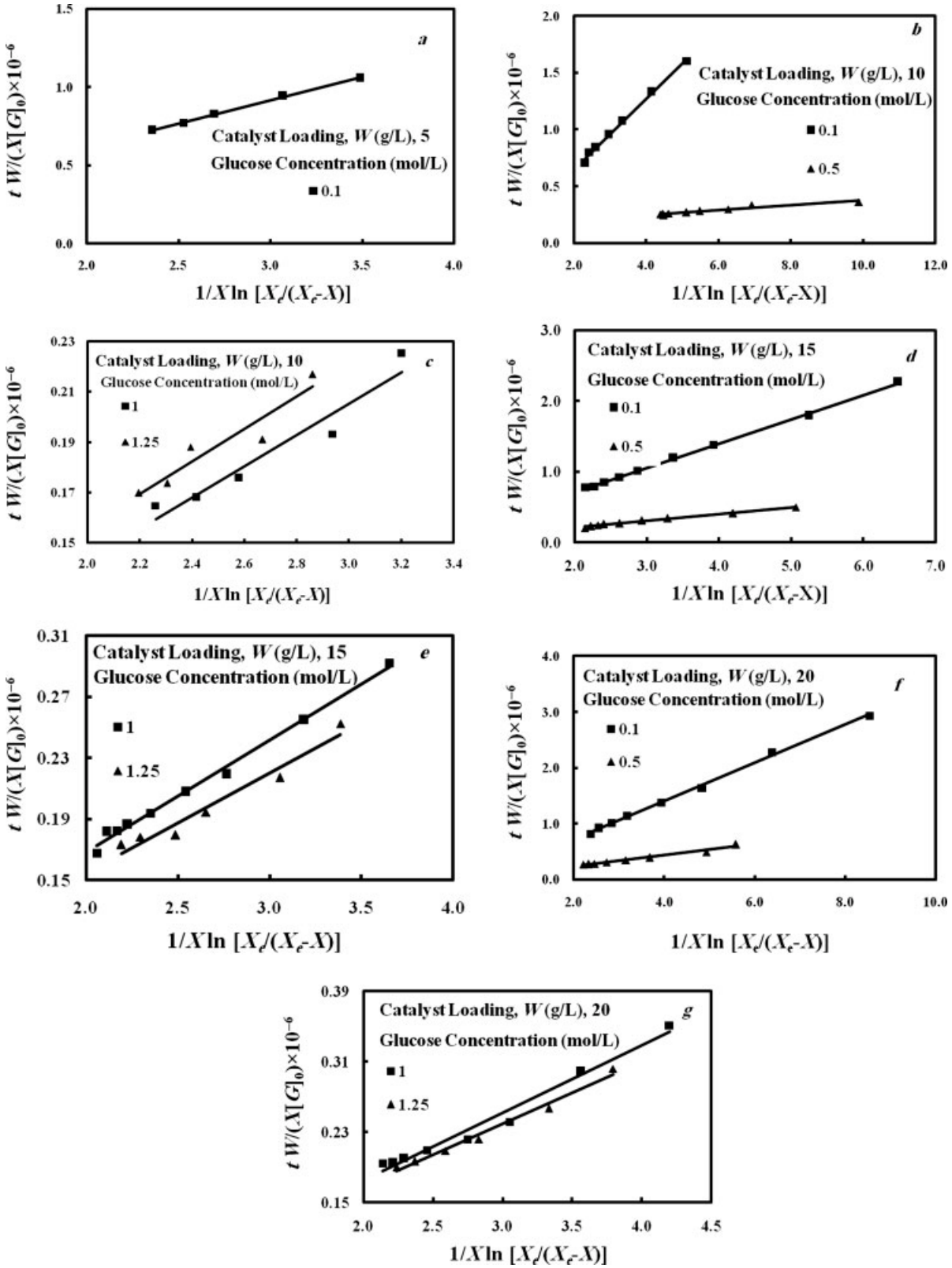

Figure 3. Variations of $tW/(X[G]_0)$ with $\ln[X_e/(X_e - X)]/X$.

Table 3. Kinetic Constants of Eq. 8

$[G]_0$ (mol/m^3)	K	K_r [10^6 mol/(g cat s)]
100	−0.070	2.991
500	−0.206	9.390
1000	−0.244	11.460
1250	−0.335	12.530

Packed-Bed Reactor Experimental Runs. In each experimental run, the feed solution at the desired temperature (60°C), with the desired inlet glucose concentration and pH was fed to the packed-bed reactor at given volumetric flow rate, while hot water was introduced into the jacket to maintain the temperature of the reactor at 60°C. The samples were taken through the sampling connection of the effluent stream of the reactor for the measurement. Experimental runs were conducted at four different flow rates (*Re* number) and four different initial concentrations of glucose. The range of operating conditions is presented in Table 2. The procedure for analysis of samples was the same as that for batch experimental runs.

Results and Discussion

Evaluation of kinetic parameters

Figures 2a–c demonstrate typical experimental data regarding the kinetic behavior of glucose to fructose reaction. As may be noticed, slight deviations from Michaelis–Menten kinetic model at low fractional conversions are observed which are shown by the rectangles. In fact a sinusoidal shape at fractional conversions <15% particularly for small values of

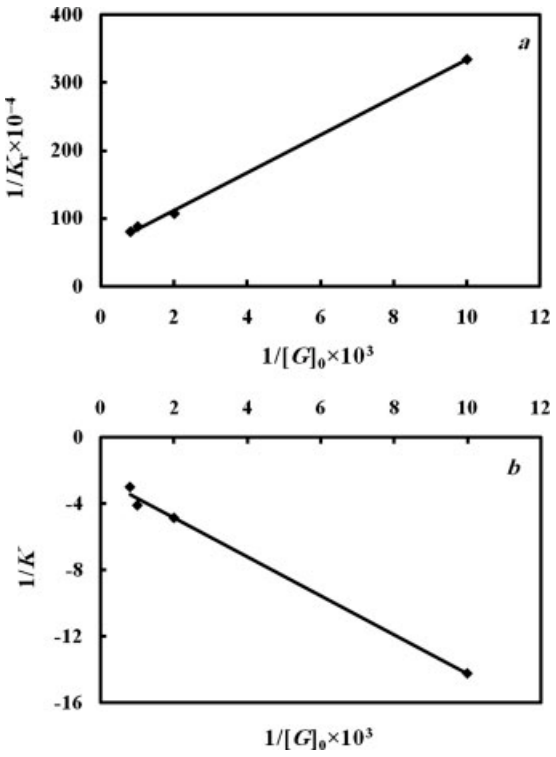

Figure 4. Variations of $1/K_r$ and $1/K$ with $1/[G]_0$.

Table 4. Kinetic Parameters of Eq. 2

k_{mg} (mol/m^3)	k_{mf} (mol/m^3)	v_{mg} [10^6 mol/(g cat s)]	v_{mf} [10^6 mol/(g cat s)]
474.3	793.9	8.869	14.910

$W/[G]_0$ is clearly visible. As fractional conversion increases, however, this sinusoidal shape is vanished and the fractional conversion curve perfectly matches with the Michaelis–Menten kinetic model. This kind of deviation has been reported formerly in the literature.[25] This behavior may be caused by a transitory behavior of the particles reflecting the time needed for the establishment of steady concentration profiles within the particles. These disturbances prevented us from relying on the initial rate of reaction to use Lineweaver–Menten method for calculating the kinetic parameters. Using the method mentioned earlier, one can easily omit these initial points and estimate kinetic parameters using the higher conversion experimental data. Moreover, using the method explained in the theoretical section, it is not necessary to conduct experimental runs with feed solutions containing only fructose to estimate v_{mf} and k_{mf}. To obtain the kinetic parameters K and K_r, the experimental data concerning $tW/(X[G]_0)$ were plotted against $1/X\ \ln[X_e/(X_e - X)]$ as shown in Figures 3a–g. From these figures, the kinetic parameters K and K_r could be evaluated by linear regression analysis. Results are summarized in Table 3. In addition, the equilibrium fractional conversion of glucose was experimentally obtained to be 49.9% and the equilibrium constant of the reaction was calculated by Eq. 6 to be 0.996.

With these values of K and K_r, one can easily evaluate the four key kinetic parameters, i.e. k_{mg}, k_{mf}, v_{mg}, and v_{mf}. To achieve this goal, the obtained values of $1/K_r$ and $1/K$ could be plotted against $1/[G]_0$ as shown in Figures 4a,b. Using the linear regression analysis, the four key kinetic parameters were found and were summarized in Table 4.

To show the goodness of the kinetic model parameters obtained by this procedure, the predicted fractional conversion of glucose using the obtained kinetic parameters is compared with the batch experimental data in Figures 5a–d and 6. As may be observed from these figures, there is a fair agreement between the experimental and predicted fractional conversions of glucose. In addition, to quantify the deviation between the predicted and experimental results, the root mean square (RMS) of the normalized residuals was calculated according to the following expression:

$$\mathrm{RMS} = 100\sqrt{\frac{1}{N}\sum_{i=1}^{N}\left(1 - \frac{X_i(\mathrm{cal})}{X_i(\mathrm{exp})}\right)^2} \qquad (28)$$

The RMS of the predicted values of fractional conversion of glucose was calculated to be 14.94%. This value of RMS clearly shows the goodness of the kinetic model. It should also be noted that in Figures 5b–d the results of experiments for 5 g/L of catalyst were not used to adjust the parameters of the proposed model, because these experiments resulted in the low conversions after 2 h and, hence, most of the data points were in the range of fluctuations. As explained earlier, the deviations from the Michaelis–Menten rate expression is observed for this fluctuation range; therefore, these results

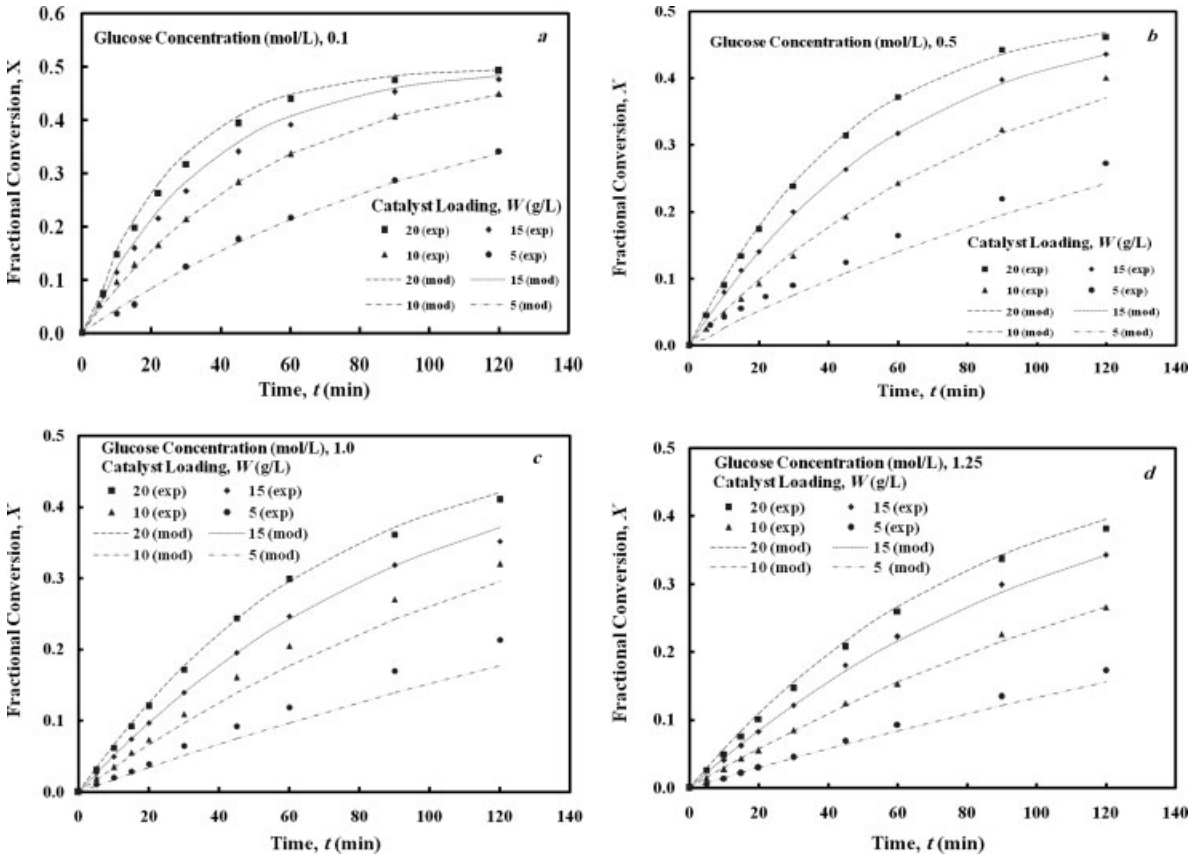

Figure 5. Variations of fractional conversion of glucose with time for batch experiments and comparison with the kinetic model predictions.

were not reliable enough to be used for the adjustment of the model parameters. Considering the earlier facts, the results of experiments with 5 g/L of IGI catalyst in Figures 5b–d could not be used for the estimation of RMS and therefore the exclusion of these data points would result in much lower values of RMS (~6%).

Packed-bed runs

Packed-bed reactor experiments were carried out using the experimental set up shown in Figure 1. The feed solution with a known concentration of glucose and at 60°C was continuously fed to the top of the column at a given volumetric flow rate. The feed flow rate was regulated by means of a rotameter. The temperature of the reactor was kept constant at 60°C by hot water introduced into the jacket. For all the column tests, the samples from the reactor effluent were intermittently taken and analyzed by HPLC. The packed bed runs were carried out at four different inlet glucose concentrations [(100, 470, 880, and 1100) mol/m^3], and four different *Re* numbers for each inlet concentration of glucose. To simulate the experimental conditions of packed-bed reactor, the axial dispersion coefficient, D_L, molecular diffusivity, D_m, and physical properties of the feed solution at 60°C should be known. The density and viscosity of feed solution were measured and the molecular diffusivity of glucose at 60°C was found elsewhere.[26] The axial dispersion coefficient may be estimated by using reported correlations. The following correlation was proposed by Fried[27] to model dispersion effects:

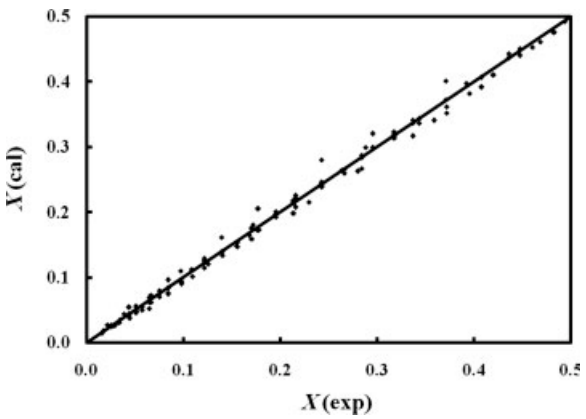

Figure 6. Comparison of calculated fractional conversions of glucose with experimental ones.

Table 5. Physical Properties at 60°C

Inlet Glucose Concentration (mol/m^3)	ρ (kg/m^3)	μ (10^4 kg/(m s)]	D_m (10^9 m^2/s)
100	987.2	7.8	1.046
470	1008.5	8.1	1.225
880	1039.2	8.5	1.439
1100	1054.2	8.8	1.604

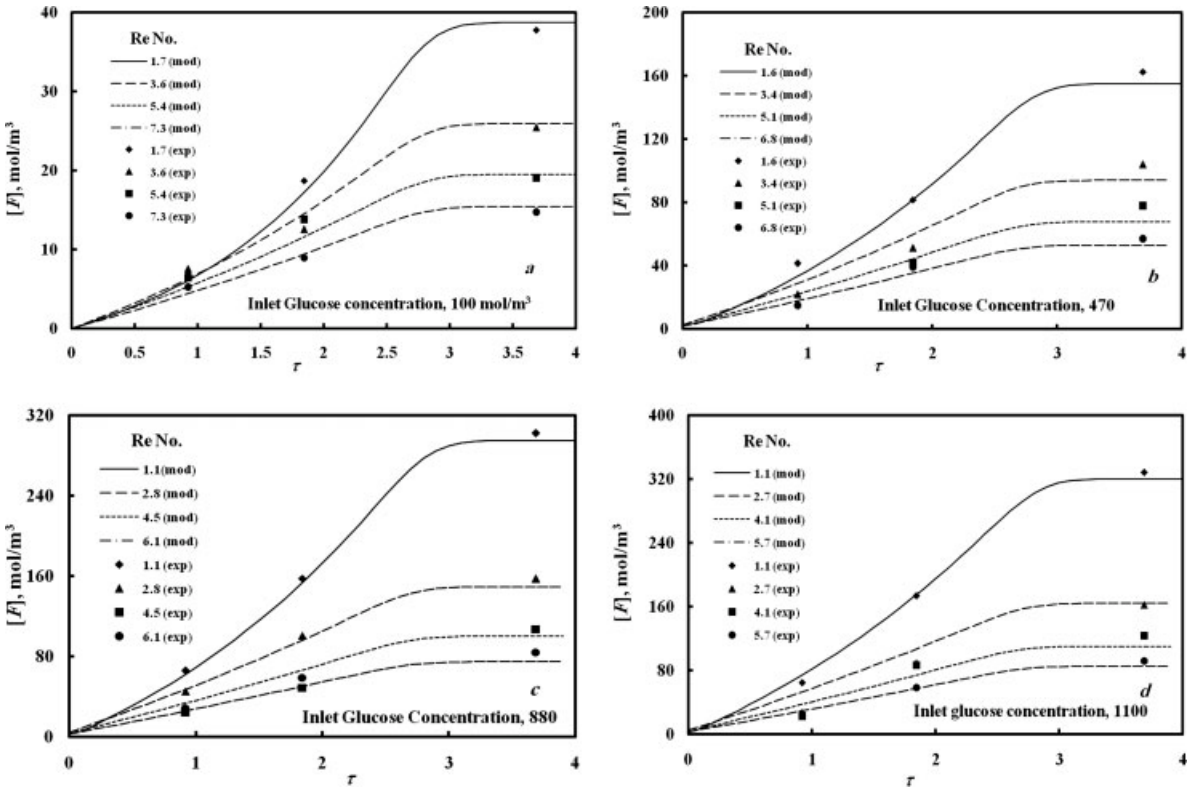

Figure 7. Variations of transient outlet concentration of fructose with dimensionless time for packed-bed reactor.

$$D_L = D_m\left[0.67 + 0.5(Re\ Sc)^{1.2}\right] \tag{29}$$

The parameters used in the simulation studies are summarized in Table 5.

The effects of particle *Re* number, and inlet glucose concentration on the concentration profile of fructose were investigated. The simulation and experimental results in terms of fructose concentration, [F], and as a function of particle *Re* number are presented in Figures 7a–d. As shown in Figures 7a–d, there are fair agreements between the experimental results and those predicted by the model.

Effect of particle Re *number*

Figure 8 shows the variations of steady state fractional conversion of glucose both experimental data and model predictions with the particle *Re* number as a function of the inlet glucose concentration. As may be noticed form Figure 8, with an increase in the particle *Re* number the steady state fractional conversion of glucose decreases. This behavior is expected and can be explained by a decrease in the mean residence time of the liquid in the bed.

Effect of axial mixing

The importance of dispersion term in reactor modeling is usually considered by determining the axial peclet number (Pe_a), which is a representation of the ratio between the rate of transport by convection and that by axial diffusion:

$$Pe_a = \frac{U_0 L}{D_L} \tag{30}$$

The high values of the axial peclet number show that convection predominates on diffusion and dispersion phenomena, whereas low values of Pe_a indicate that axial mixing occurs in the axial direction. Other authors have stipulated conditions that are required to be satisfied in order to exclude the axial mixing term in the material and energy balance equa-

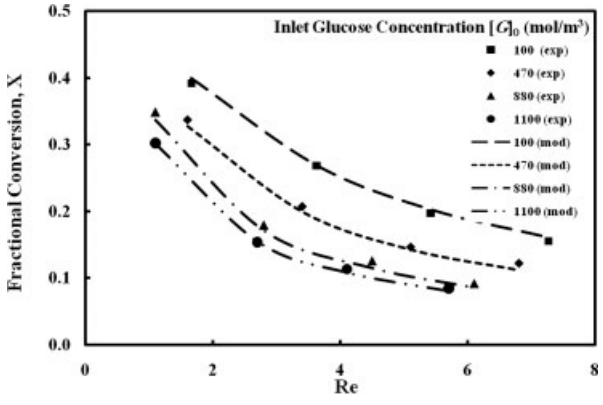

Figure 8. Variations of steady-state fractional conversion of glucose with particle *Re* number for packed-bed reactor.

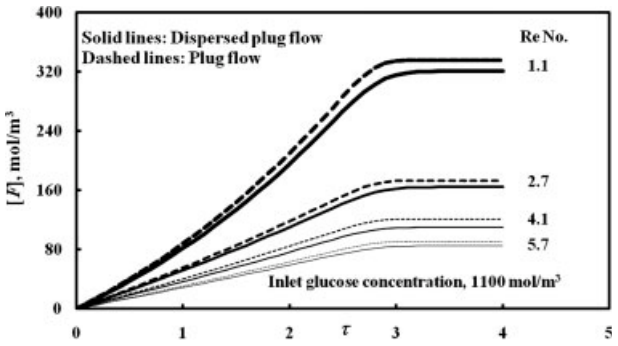

Figure 9. Effect of axial mixing term on the performance of the fixed-bed reactor.

tions for a packed-bad catalytic tubular reactor. For example, Hill,[28] Carberry and Wendel[29] suggested that if the ratio of catalyst bed length to the catalyst particle diameter (L/d_p) is larger than 100, the axial mixing term will be negligible. Also, Froment and Bischoff[30] and Rase[31] suggested that the effect of the axial mixing term is negligible when $L/d_p > 50$ and $d_b/d_p > 10$. To evaluate the applicability of these criteria in the glucose to fructose reaction, we have solved the governing equations together with the initial and boundary conditions with and without the axial dispersion term. The model predictions are plotted in Figure 9 as a function of the particle *Re* number for a given inlet glucose concentration (1100 mol/m^3), where the solid lines represent the model predictions with the axial mixing term (dispersed plug flow reactor), whereas the dashed lines indicate those without the axial mixing term (plug flow reactor). As may be observed from this figure, there are slight differences in the outlet fructose concentration predicted by the model with and without the axial mixing term, which goes on to support the mentioned criteria.

Effect of $\mathbf{Pe}_a$ *number*

Figure 10 shows the variations of steady state fractional conversion of glucose both experimental data and model predictions with the Pe_a number as a function of inlet glucose concentration. As may be noticed form Figure 10, with an

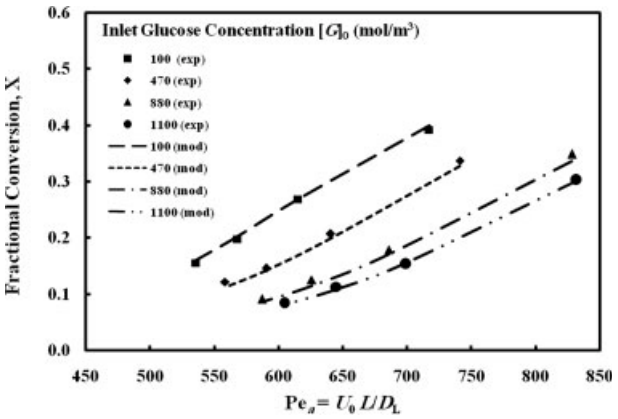

Figure 10. Effect of axial Pe_a number on the steady-state fractional conversion of glucose.

Table 6. Variations of Steady State Dimensionless Time (τ_{ss}) with *Re* Number and $[G]_0$.

$[G]_0$ (mol/m^3)	*Re*	τ_{ss}
100	1.7	3.09
100	3.6	3.02
100	5.4	3.01
100	7.3	3.00
470	1.6	3.05
470	3.4	3.00
470	5.1	2.99
470	6.8	2.99
880	1.1	3.06
880	2.8	3.00
880	4.5	2.99
880	6.1	2.98
1100	1.1	3.04
1100	2.7	3.00
1100	4.1	2.99
1100	5.7	2.98

increase in the Pe_a number the steady state fractional conversion of glucose increases. This behavior can be attributed to a decrease in the particle *Re* number, which in turn increases the Pe_a number because of the strong dependence of D_L on the *Re* number. This behavior of axial peclet number of liquid phases is expected over the low range of particle *Re* number, i.e. 1–10.[32,33]

Steady state dimensionless time (τ_{ss})

Table 6 lists the predicted values of steady state dimensionless time (τ_{ss}) for various *Re* numbers and inlet glucose concentrations. This parameter is defined as a ratio of the steady state time to the mean residence time of liquid stream in the fixed-bed reactor. The steady state time was considered as the time it takes the concentration of fructose [F] reach almost the final steady state value with $\Delta[F] \leq 1\%$. As may be noticed, the values of τ_{ss} do not appreciably vary with the *Re* number and inlet glucose concentration. This behavior shows that an increase in the *Re* number, i.e. decrease in the mean residence time of liquid stream, results in a decrease in the steady state time (t_{ss}) in such way that the value of $t_{ss} \times Re$ remains almost constant. In addition, the system behaves in such way that the variations of inlet glucose concentration do not significantly affect of τ_{ss} for the range of operating conditions investigated in the present work.

Conclusions

An experimental and theoretical investigation was conducted on the kinetics, dynamic modeling, and simulation of isomerization reaction of D-glucose to D-fructose using commercial IGI catalyst, Sweetzyme type IT. The kinetic parameters of the reaction were determined by analysis of experimental data through the Michaelis–Menten kinetics. From batch experimental runs, it was founds that:

(1) The equilibrium fractional conversion of D-glucose to D-fructose at 60°C is 49.9%.

(2) It was observed that there are some slight deviations from the Michaelis–Menten kinetic model at low fractional conversions as reported previously by Benaiges et al.[25] But,

as the fractional conversion is increased the experimental results perfectly match the Michaelis–Menten kinetic model.

(3) The parameters of the kinetic model of glucose to fructose reaction could be evaluated by the procedure described in the present work.

The packed-bed reactor was dynamically modeled by the dispersed-phase model, and it was observed that there are fair agreements between the experimental data and those predicted by the model at various inlet glucose concentrations and particle *Re* number. Moreover, it was found that the effect of axial mixing on the performance capability of the packed-bed reactor over the range of operating conditions investigated in the present work is negligible.

Notation

d_p = particle diameter, m
d_b = bed diameter, m
D_L = dispersion coefficient, m^2/s
D_m = molecular diffusion coefficient, m^2/s
E = enzyme concentration, mol/m^3
[F] = concentration of fructose, mol/m^3
$[F]_0$ = initial or inlet concentration of fructose, mol/m^3
$[F]_e$ = equilibrium concentration of fructose, mol/m^3
[G] = concentration of glucose, mol/m^3
$[G]_e$ = equilibrium concentration of glucose, mol/m^3
$[G]_0$ = initial or inlet concentration of glucose, mol/m^3
$[\overline{G}]$ = concentration of glucose, Eq. 3
$[\overline{G}]_0$ = concentration of glucose ($[G]_0 - [G]_e$)
GE = intermediate complex, Eq. 1
K = kinetic constant, Eq. 10
K_e = equilibrium constant, Eq. 6
K_m = apparent Michaelis–Menten constant, Eq. 4, mol/m^3
K_r = kinetic constant, Eq. 9, mol/(g cat s)
k_{mf} = Michaelis–Menten constant for fructose, mol/m^3
k_{mg} = Michaelis–Menten constant for glucose, mol/m^3
L = height of reactor, m
Pe_a = axial peclect number ($=U_0L/D_L$)
R = reaction rate, mol/(g cat s)
Re = particle Reynolds number ($=\rho U_0 d_p/\mu$)
Sc = Schmidt number ($=\mu/(\rho D_m)$
t = time, s
t_{ss} = steady state time, s
U_0 = superficial velocity, m/s
V_m = maximum apparent reaction rate, Eq. 5, mol/(g cat s)
v_{mf} = maximum apparent reaction rate for fructose, mol/(g cat s)
v_{mg} = maximum apparent reaction rate for glucose, mol/(g cat s)
W = immobilized catalyst loading, g/L
X = fractional conversion of glucose
X_e = equilibrium fractional conversion of glucose
z = axial distance, m

Greek letters

ε = void fraction of bed
τ = dimensionless time, Eq. 19
τ_{ss} = steady state dimensionless time
ξ = dimensionless axial distance, Eq. 19
ρ = fluid density, kg/m^3
ρ_p = catalyst particle density, kg/m^3
μ = fluid viscosity, kg/(m s)
Δ = difference

Abbreviations

cal = calculated
cat = catalyst
exp = experimental
mod = model

Acknowledgments

The authors gratefully acknowledge Novo Nordisk (Iran) for providing IGI catalyst, Sharif University of Technology for providing financial support, and Professor F. Khorasheh for useful comments.

Literature Cited

1. Dehkordi AM. Novel type of two-impinging-jets reactor for solid–liquid enzyme reactions. *AIChE J*. 2006;52:692–704.
2. Asif M, Abasaeed AE. Modeling of glucose isomerization in a fluidized bed immobilized enzyme bioreactor. *Bioresour Technol*. 1998; 64:229–235.
3. Bravo V, Jurado E, Luzon G, Cruz N. Kinetics of fructose–glucose isomerization with Sweetzyme type A. *Can J Chem Eng*. 1998; 76:778–783.
4. Faqir NM, Attarakih MM. Optimal temperature policy for immobilized enzyme packed bed reactor performing reversible Michaelis–Menten kinetics using the disjoint policy. *Biotechnol Bioeng*. 2002; 77:163–173.
5. Haas WR, Tavlarides LL, Wnek W. Optimal temperature policy for reversible reactions with deactivation: applied to enzyme reactors. *AIChE J*. 1974;20:707–712.
6. Lee HS, Hong J. Kinetics of glucose isomerization to fructose by immobilized glucose isomerase: anomeric reactivity of D-glucose in kinetic model. *J Biotechnol*. 2000;84:145–153.
7. Messing RA, Filbert AM. An immobilized glucose isomerase for the continuous conversion of glucose to fructose. *J Agric Food Chem*. 1975;23:920–923.
8. Palazzi E, Converti A. Generalized linearization of kinetics of glucose isomerization to fructose by immobilized glucose isomerase. *Biotechnol Bioeng*. 1999;63:273–284.
9. Palazzi E, Converti A. Evaluation of diffusional resistances in the process of glucose isomerization to fructose by immobilized glucose isomerase. *Enzyme Microb Technol*. 2001;28:246–252.
10. Straatsma J, Vellenga K, de Willt HGJ, Joosten GEH. Isomerization of glucose to fructose, Part 1: The stability of a whole cell immobilized glucose isomerase catalyst. *Ind Eng Chem Process Des Dev*. 1983;22:349–356.
11. Straatsma J, Vellenga K, de Willt HGJ, Joosten GEH. Isomerization of glucose to fructose, Part 2: Optimization of reaction conditions in the production of high fructose syrup by isomerization of glucose catalyzed by a whole cell immobilized glucose isomerase catalyst. *Ind Eng Chem Process Des Dev*. 1983;22:356–361.
12. Khorasheh F, Kheirolomoom A, Mireshghi S. Application of an optimization algorithm for estimating intrinsic kinetic parameters of immobilized enzymes. *J Biosci Bioeng*. 2002;94:1–7.
13. Toumi A, Engell S. Optimization-based control of a reactive simulated moving bed process for glucose isomerization. *Chem Eng Sci* 2004;59:3777–3792.
14. Vilonen KM, Vuolanto A, Jokela J, Leisola MSA, Krause AOI. Enhanced glucose to fructose conversion in acetone with xylose isomerase stabilized by crystallization and cross-linking. *Biotechnol Prog*. 2004;20:1555–1560.
15. Zhang Y, Hidajat K, Ray AK. Optimal design and operation of SMB bioreactor: production of high fructose syrup by isomerization of glucose. *Biochem Eng J*. 2004;21:111–121.
16. Bailey JE, Ollis DF. *Biochemical Engineering Fundamentals*, 2nd ed. New York, NY: McGraw-Hill, 1986.
17. da Silva EAB, de Souaza AAU, de Souza SGU, Rodrigues AE. Analysis of the high-fructose syrup production using reactive SMB technology. *Chem Eng J*. 2006;118:167–181.
18. Hong J, Yu H, Chen K. Analysis of substrate protection of an immobilized glucose isomerase reactor. *Biotechnol Bioeng*. 1993;41:451–458.
19. Racki DV, Pavlovic N, Cizmek S, Drazic M, Husadzic B. Development of reactor model for glucose isomerization catalyzed by whole-cell immobilized glucose isomerase. *Bioprocess Eng*. 1991;7:183–187.
20. Kikkert A, Vellenga K, De wilt HGJ, Joosten GEH. The isomerization of D-glucose into D-fructose catalyzed by whole-cell immobilized glucose isomerase. The dependence of the intrinsic rate of reaction on substrate concentration, pH and temperature. *Biotechnol Bioeng*. 1981;23:1087–1101.

21. Rubio FC, Alalmeda EJ, Tello PG, Gonzalez GL. Kinetic study of fructose–glucose isomerization in a recirculation reactor. *Can J Chem Eng*. 1995;73:935–940.
22. Lee YY, Fratzke AR, Wun K, Tsao GT. Glucose isomerase immobilized on porous glass. *Biotechnol Bioeng*. 1976;18:389–413.
23. Illanes A, Zungia M, Contreras S, Guerrero A. Reactor design for enzymatic isomerization of glucose to fructose. *Bioprocess Eng*. 1992;7:199–204.
24. Illanes A, Wilson L, Raiman L. Design of immobilized enzyme reactors for the continuous production of fructose syrup from whey permeate. *Bioprocess Eng*. 1999;21:509–515.
25. Benaiges MD, Sola C, de Mas C. Instrinsic kinetic constant of an immobilized glucose–isomerase. *J Chem Technol Biotechnol*. 1986; 36:480–486.
26. Robert CW. *CRC Handbook of Chemistry and Physics*, *68th ed*. Boca Raton, Florida: CRC Press, 1987–1988.
27. Fried JJ. *Groundwater Pollution*. Amsterdam, The Netherland: Elsevier, 1975.
28. Hill CG. *An Introduction to Chemical Engineering Kinetics and Reactor Design*. New York: Wiley, 1977.
29. Carberry JJ, Wendel MM. A computer model of the fixed bed catalytic reactor: the adiabatic and quasi-adiabatic cases. *AIChE J*. 1963;9:129–133.
30. Froment GF, Bischoff KB. *Chemical Reactor Analysis and Design*. New York: Wiley, 1990.
31. Rase HF. *Chemical Reactor Design for Process Plants*. New York: Wiley, 1987.
32. Carberry JJ. *Chemical and Catalytic Reaction Engineering*. New York: McGraw-Hill, 1976.
33. Nauman EB. *Chemical Reactor Design, Optimization, and Scale Up*. New York: McGraw-Hill, 2002.

Manuscript received Oct. 24, 2007, and revision received Jan. 21, 2008.